

surface it was no longer possible to obtain oriented crystals. Using an optical cryostat we have confirmed this, by observing the orientation of ^4He crystals nucleated on clean Grafoil (Fig. 4). For other materials, both Landau *et al.*¹¹ and Balibar, Castaing, and Laroche¹⁴ found that single hcp crystals do not generally wet copper or glass as well as the superfluid ^4He does (contact angle $> 90^\circ$). It will be very interesting if clean single crystals of MgO nucleate oriented bcc ^3He crystals.

In conclusion, we should reemphasize the analogy to the adsorption results from the vapor phase. As in the case of hcp ^4He on Grafoil we now find that bcc ^3He on MgO belongs to the class I category of Dash¹⁵ and Peierls.¹⁶

We acknowledge useful discussions with S. Alexander, J. G. Dash, D. O. Edwards, M. Bretz, and H. Wiechert. We thank Y. Lahav for his technical assistance.

¹J. Landau and W. F. Saam, *Phys. Rev. Lett.* **38**, 23 (1977).

²J. Landau and Y. Eckstein, *Phys. Rev. Lett.* **42**, 67 (1979); Y. Eckstein and J. Landau, to be published.

³The MgO "smoke" was generously provided by Professor J. G. Dash.

⁴J. G. Dash, R. Ecke, J. Stoltenberg, O. E. Vilches, and O. J. Whitmore, Jr., *J. Phys. Chem.* **82**, 1450 (1978).

⁵M. Nielson, J. P. McTague, and W. Ellenson, *J. Phys. (Paris), Colloq.* **38**, C4-1 (1977); K. Carneiro, *J. Phys. (Paris), Colloq.* **38**, C4-1 (1977).

⁶Isopycnals are lines in a P, T diagram defined by a constant-volume system containing a constant number of atoms. On a microscopic scale, however, the density of the helium varies as a function of z , the distance from the substrate. See Ref. 1 for a detailed discussion.

⁷G. C. Straty and E. D. Adams, *Rev. Sci. Instrum.* **40**, 1393 (1969).

⁸Y. Eckstein, Y. Lahav, J. Landau, and Z. Olami, *Phys. Lett.* **76A**, 77 (1980).

⁹M. Bienfait, J. G. Dash, and J. Stoltenberg, *Phys. Rev. B* **21**, 2765 (1980).

¹⁰J. E. Avron, L. S. Balfour, C. G. Kuper, J. Landau, S. G. Lipson, and L. S. Schulman, *Phys. Rev. Lett.* **45**, 814 (1980).

¹¹J. Landau, S. G. Lipson, L. M. Määttänen, L. S. Balfour, and D. O. Edwards, *Phys. Rev. Lett.* **45**, 31 (1980).

¹²Estimates show that the geometrical parameters can cause this coefficient to vary by as much as a factor of 2.

¹³H. Wiechert, H. J. Lauter, and B. Stühn, to be published.

¹⁴S. Balibar, B. Castaing, and C. Laroche, *J. Phys. (Paris), Lett.* **41**, L283 (1980).

¹⁵J. G. Dash, *Phys. Rev. B* **15**, 3136 (1977).

¹⁶Rudolph Peierls, *Phys. Rev. B* **18**, 2013 (1978).

Distance-Dependent Relaxation Shifts of Photoemission and Auger Energies for Xe on Pd(001)

G. Kaindl,^(a) T.-C. Chiang, D. E. Eastman, and F. J. Himpsel

IBM Thomas J. Watson Research Center, Yorktown Heights, New York 10598

(Received 28 March 1980)

Photoelectrons and Auger electrons from Xe in adsorbed multilayers of Xe on Pd(001) as well as on spacer layers of Kr on Pd(001) exhibit well-resolved increases in kinetic energy with decreasing distance from the surface (2–28 Å), allowing a direct labeling of the layers. These relaxation shifts for core-hole excitations (0.9–2.1 eV) and for Auger excitations (3.3–6.6 eV) are well described by an image potential, where the position of the image plane agrees within 0.2 Å with local-density functional theory.

PACS numbers: 79.60.Gs

Core-level binding energies and Auger electron energies for adsorbates are shifted relative to their free-atom counterparts by initial-state potential-energy effects and by hole-relaxation (polarization) effects. For physisorbed species on metals, relaxation effects due to the screening of excited hole states by the metal surface are of central importance. Extensive theoretical work on single-hole and two-hole relaxation effects has

been reported¹⁻⁵ but no clear-cut experimental tests have been performed, in part because of the difficulty of separating initial-state and final-state effects. In this respect, rare-gas atoms are especially attractive in that initial-state chemical effects are expected to be minimal. To date, however, rare-gas core-level binding energy shifts have only been studied for atoms implanted in metals⁶ and semiconductors,⁷ for which initial-

state effects are believed to be significant. X-ray core-level binding energy shifts for monolayers and multilayers of adsorbed SF_6 on Ru,⁸ as well as $5p_{3/2,1/2}$ binding energies for Xe adsorbed on Pd(110)⁹ in the zero to one monolayer range, have been reported.

The present Letter reports on the observation of well-resolved energy shifts for photoelectrons and Auger electrons emitted from Xe atoms adsorbed on Pd(001) at distances in the range 2–28 Å from the surface. Varying distances are achieved by adsorbing Xe atoms directly on Pd(001) as well as on dielectric spacers of monolayers, bilayers, and multilayers of Xe and Kr. For these adsorbate configurations, distance-dependent single-hole binding-energy shifts of 0.9–2.1 eV and Auger-energy shifts of 3.3–6.6 eV relative to the free-atom energies are observed. The observation that the Xe-*NOO* Auger energy shifts are 3 times larger than those of the 4*d* photoelectron (PE) lines implies that full metallic screening of the initial core-hole and of the final two-hole state occurs in the Auger process, and that only relatively small initial-state potential energy effects contribute. For localized excitations (Xe-4*d* and Xe-*NOO* Auger levels), the distance-dependent shifts are well described by a point-charge image-potential model, where the image plane agrees within 0.2 Å with the results of local-density functional theory. The observed shifts provide a new and straightforward method for distinguishing, i.e., labeling, adsorbed rare-gas atoms in the different layers.

The data were taken with a double-cylindrical mirror analyzer system and toroidal grating monochromator at the Synchrotron Radiation Center of the University of Wisconsin. The temperature of the Pd(001) crystal (cleaned by Ar sputtering and annealing) could be varied continuously between 40 and 1100 K by use of a sample heater and a closed-cycle helium refrigerator. Rare gases were adsorbed at a substrate temperature of 40 K, and close-packed monolayers of both Xe and Kr were formed by depositing slightly thicker layers and then annealing at a temperature below the monolayer temperature but above the second-layer desorption temperature. Bilayers of Xe and Kr were formed by the same method. Because of the large distance-dependent core-level shifts, this process can be followed in a quantitative way via the core-level emission intensities of first- and second-layer atoms.

Figure 1 shows angle-integrated Xe-4*d* PE spectra and Xe-*NOO* Auger spectra for various Xe

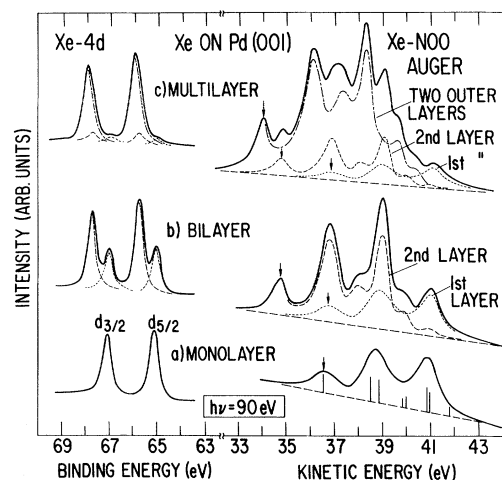


FIG. 1. Xe-4*d* PE spectra and Xe-*NOO* Auger spectra for (a) a monolayer, (b) a bilayer, and (c) a multilayer (four layers) of Xe on Pd(001). The bilayer and multilayer spectra are decomposed into contributions from the first, the second, and the two unresolved outer layers. In the monolayer Auger spectrum the relative positions and intensities of the individual *NOO* components from gas-phase Xe data (Ref. 10) are represented by vertical bars. The splitting of the lowest-kinetic-energy *NOO* Auger component is indicated by arrows. The statistical uncertainty of the data is less than twice the linewidth of the drawing.

configurations on Pd(001). For a monolayer-Xe coverage, the Xe-4*d* spectrum exhibits a spin-orbit splitting of 1.98 ± 0.02 eV, in agreement with the free-atom value. The 4*d* binding energies (relative to the vacuum level) are found to be 2.14 eV smaller than for the free atom, caused mainly by metallic screening of the final-state core hole. For a bilayer-Xe coverage, two well-resolved sets of Xe-4*d* peaks split by 0.72 ± 0.03 eV are observed. The less-intense set stems from the underlayer (first layer), while the more intense one originates from the overlayer (second layer). For a multilayer-Xe film (four layers) the 4*d* spectrum exhibits contributions from all the differently spaced layers, with relative intensities determined by the electron escape depth.

The same observations are made with the Xe-*NOO* Auger spectra, but the changes in kinetic energy are 3 times the equivalent 4*d* binding energy shifts (within 5%). The bilayer Auger spectrum [Fig. 1(b)] consists of two sets of Auger lines. The second-layer contribution, shifted by 2.01 ± 0.05 eV towards lower kinetic energies with respect to the first-layer contribution, is obtained by subtracting the monolayer spectrum of Fig. 1(a) (short-dashed line) from the meas-

TABLE I. Xe-5*p* and Xe-4*d* binding energy shifts ΔE_B and Xe-*NOO* Auger kinetic-energy shifts ΔE_K relative to free atoms for Xe overlayers on Pd(001). All binding energies were measured relative to the (coverage-dependent) vacuum level and are given in eV. The error bars for the quoted numbers are estimated to be ± 0.05 eV.

Xe configuration	Layer	ΔE_B (5 <i>p</i>)	ΔE_B (4 <i>d</i>)	ΔE_K
Monolayer	1st	-1.71	-2.14	6.57
	Bilayer	-1.69	-2.21	6.70
Multilayer	2nd	-1.10	-1.49	4.69
	1st	...	-2.24	6.79
	2nd	...	-1.54	4.75
	outer	-0.90 ^a	-1.28 ^b	4.89

^a Five layers of Xe.

^b Four layers of Xe.

ured bilayer spectrum. To this end, the monolayer spectrum has to be shifted by 0.13 eV to higher kinetic energies. This small shift of the underlayer contribution relative to the monolayer spectrum is caused by additional dielectric screening of the core hole by the Xe overlayer. This effect is also observed in the 4*d*-PE spectra (see Table I). In Fig. 1(c) the multilayer-Xe Auger spectrum is decomposed in the same way into separate contributions from the first, the second, and the two unresolved outer layers. The monolayer spectrum [Fig. 1(a)] is broadened as compared to the second- and the outer-layer contributions; this may be due to inhomogeneity effects of the Pd(001) surface on the incommensurate overlayer.^{11, 12}

Well-resolved distance-dependent shifts are also observed in the Xe-5*p* PE spectra, but the resulting shifts are found to be about 30% smaller than the equivalent 4*d* shifts. The results of our analysis for the Xe configurations studied are summarized in Table I.

In addition, we have studied the distance-dependent shifts for Xe atoms adsorbed on Kr-covered Pd(001). In this way, single-layer PE and Auger spectra are observed (Fig. 2), which are shifted according to the number of Kr layers used as the dielectric spacer. In both the monolayer-Kr and the bilayer-Kr spectra, small additional components due to Xe atoms adsorbed directly on the Pd(001) surface and on top of the first Kr layer, respectively, are observed. They originate from Xe atoms which have penetrated the Kr spacer layers. This effect can be used for studying rare-gas diffusion on a metal surface.

The observed distance-dependent shifts for lo-

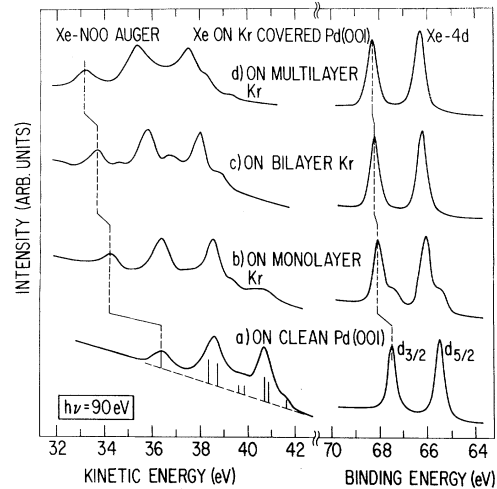


FIG. 2. Xe-*NOO* Auger and Xe-4*d* PE spectra of a submonolayer of Xe (about one-half of a monolayer) adsorbed on Kr films of various thicknesses on Pd(001).

calized excitations (Xe-4*d* and Xe-*NOO* Auger) can be described in terms of hole-relaxation effects for adsorbed atoms on a metal surface using a point-charge image-potential model. In this model, the interaction of a core hole of charge q at a distance d from the metal surface (i.e., the "jellium" edge, which is defined to be one-half of an interplanar distance outside of the last plane of ions) is given by a potential of the form $-q^2/[4(d-x_0)]$, as has been theoretically described.¹⁻³ The position of the image plane (center of mass of the induced surface charge distribution) is located at x_0 outside of the metal surface, with a value of $x_0 = 0.85$ Å resulting from jellium-model calculations for an electron density ($r_s = 2$) corresponding to Pd.¹³ For monolayer-Xe coverage, we have calculated $d = 2.38$ Å as the mean distance of an incommensurate Xe overlayer from the Pd(001) surface, using a hard-sphere model with radii taken from the lattice constants of rare-gas solids and bulk Pd metal.¹⁴ For thicker layers, the distances d were calculated assuming close-packed ordered layer structures. The dielectric effects of rare-gas underlayers on the relaxation shifts were described by a homogeneous dielectric slab with dielectric constant ϵ ($\epsilon = 2.25$ for Xe and 1.90 for Kr) extending from the image plane to a distance $d - x_d$ from the metal surface.

The experimental values for the Xe-4*d* and the Xe-5*p* PE line shifts as well as the *NOO* Auger shifts (divided by 3) are plotted in Fig. 3 as a function of $1/d$. The dotted line represents the results of our semiclassical model for the Xe-4*d*

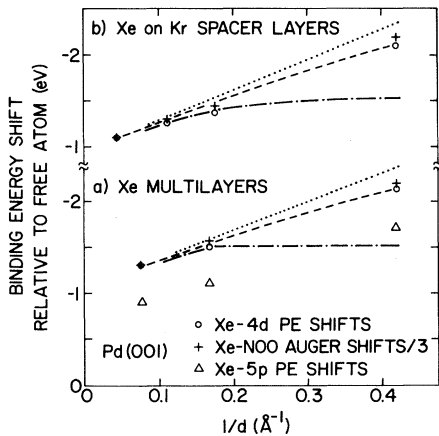


FIG. 3. Plot of Xe-4d and Xe-5p PE shifts and Xe-NOO Auger shifts (divided by 3) as a function of reciprocal distance $1/d$ from the Pd(001) surface; (a) for Xe multilayers and (b) for submonolayer Xe on top of Kr spacer layers. The right-most data points correspond to first-layer Xe on Pd(001). The results of our semiclassical model are represented by dashed lines for $x_0 = 0.68 \text{ \AA}$, by dotted lines for $x_0 = 0.85 \text{ \AA}$, and by dash-dotted lines for $x_0 = 0$ (classical case), where x_0 is the image-plane distance beyond the classical lattice termination plane (see text).

shifts using $x_0 = 0.85 \text{ \AA}$ for Pd, as given by local-density functional theory,² and fitting $x_d = 1.29 \text{ \AA}$ (1.18 \AA) to the observed shifts for the outer layers in the case of Fig. 3(a) [Fig. 3(b)], respectively. The latter is justified because initial-state effects are expected to be negligible for the outer layers. Our one-parameter model describes the experimental points rather well except for the first-layer value. This small deviation can be due to an initial-state shift for first-layer Xe atoms of 0.1–0.2 eV, as estimated from the measured decrease in substrate work function for a monolayer coverage of Xe on Pd(001) ($\Delta\phi = -0.65 \text{ eV}$). This effect reduces the theoretical shift and would essentially eliminate the discrepancy between theory (dotted line) and experiment. If we neglect this effect and fit our model to the first-layer shifts (dashed lines in Fig. 3), we obtain $x_0 = 0.68$. We consider this to be a lower limit for x_0 . We note that a “classical” image-potential model ($x_0 = 0$), represented by the dash-dotted lines in Fig. 3, does not fit the data.

As shown in Fig. 3, the Xe-NOO Auger shifts relative to the free atom are 3 times as large (within 5%) as the corresponding Xe-4d core-hole binding energy shifts. This is readily understood

in terms of a point-charge image-potential model with full metallic screening of the initial core-hole and of the final two-hole Auger state, since the hole relaxation shift of a localized two-hole state is four times the one of a one-hole state. The fact that even for the first Xe layer a factor of 3 is observed indicates again that initial-state effects are small in the present case. As mentioned above, the 5p shifts for Xe monolayers are about 30% smaller than the Xe-4d shifts; this may be due to the bandlike character¹⁵ of the 5p states as compared to the localized 4d states.

We have also studied these distance-dependent shifts for Xe on an Al(111) substrate (\sim same r_s , but of course chemically different metal) and have obtained essentially identical results that confirm our present conclusions.

The authors acknowledge valuable contributions by A. M. Bradshaw in the initial stages of this work, as well as the support by J. J. Donelon, A. Marx, and the staff of the Synchrotron Radiation Center of the University of Wisconsin–Madison. The work was supported in part by the Air Force Office of Scientific Research under Contract No. F49620-80-C0025. One of us (G.K.) is an IBM Visiting Scientist.

^(a)Permanent address: Institut für Atom und Festkörperphysik, Freie Universität, Berlin, Germany.

¹J. A. Appelbaum and D. R. Hamann, Phys. Rev. B **6**, 1122 (1972).

²N. D. Lang and W. Kohn, Phys. Rev. B **7**, 3541 (1973).

³N. D. Lang and A. R. Williams, Phys. Rev. B **16**, 2408 (1977).

⁴N. D. Lang and A. R. Williams, Phys. Rev. B **20**, 1369 (1979).

⁵J. A. D. Matthew, Surf. Sci. **89**, 596 (1979).

⁶P. H. Citrin and D. R. Hamann, Phys. Rev. B **10**, 4948 (1974).

⁷B. J. Wacławski *et al.*, Phys. Rev. Lett. **41**, 583 (1978).

⁸Galen B. Fisher *et al.*, Surf. Sci. **65**, 210 (1977).

⁹J. Kupperts *et al.*, Surf. Sci. **88**, 1 (1979).

¹⁰L. O. Werme *et al.*, Phys. Scr. **6**, 141 (1972).

¹¹P. W. Palmberg, Surf. Sci. **25**, 598 (1971).

¹²K. Horn *et al.*, Phys. Rev. Lett. **41**, 822 (1978).

¹³V. L. Moruzzi *et al.*, *Calculated Electronic Properties of Metals* (Pergamon, New York, 1978).

¹⁴This procedure reproduces within 0.05 \AA the measured distance for the equivalent case of Xe on Ag(111): N. Stoner *et al.*, Phys. Rev. Lett. **40**, 243 (1978).

¹⁵M. Sheffler *et al.*, Surf. Sci. **80**, 69 (1979).